

# BOSS-3D: A Binary Object Spectral Synthesis Code in 3D

L. Hennicker<sup>1</sup>, N. D. Kee<sup>2</sup>, T. Shenar<sup>1,3</sup>, J. Bodensteiner<sup>1,4</sup>,  
M. Abdul-Masih<sup>5</sup>, I. El Mellah<sup>6</sup>, H. Sana<sup>1</sup> and J. O. Sundqvist<sup>1</sup>

<sup>1</sup>Institute of Astronomy, KU Leuven, Celestijnenlaan 200D, 3001 Leuven, Belgium  
email: [levin.hennicker@kuleuven.be](mailto:levin.hennicker@kuleuven.be)

<sup>2</sup>National Solar Observatory, 22 Ohi'a Ku Street, Makawao, HI 96768, USA

<sup>3</sup>Anton Pannekoek Institute for Astronomy, University of Amsterdam, Postbus 94249, 1090  
GE Amsterdam, The Netherlands

<sup>4</sup>European Southern Observatory, Karl-Schwarzschild-Strasse 2, D-85748 Garching bei  
München, Germany

<sup>5</sup>European Southern Observatory, Alonso de Cordova 3107, Vitacura, Casilla 19001, Santiago  
de Chile, Chile

<sup>6</sup>Institut de Planétologie et d'Astrophysique de Grenoble, 414 Rue de la Piscine, 38400  
Saint-Martin-d'Hères, France

**Abstract.** To decode the information stored within a spectrum, detailed modelling of the physical state is required together with accurate radiative transfer solution schemes. In the analysis of stellar spectra, the numerical model often needs to account for high velocity outflows, multi-dimensional structures, and the effects of binary companions. Focusing now on binary systems, we present the BOSS-3D spectral synthesis code, which is capable of calculating synthetic line profiles for a variety of binary systems. Assuming the state of the circumstellar material to be known, the standard *pz*-geometry is extended by defining individual coordinate systems for each object. By embedding these coordinate systems within the observer's frame, BOSS-3D automatically accounts for outflows or discs within both involved systems, and includes all Doppler shifts. Moreover, the code accounts for different length-scales, and thus could also be used to analyse transit-spectra of planetary atmospheres. As a first application of BOSS-3D, we model the phase-dependent H $\alpha$  line profiles for the enigmatic binary (or multiple) system LB-1.

**Keywords.** radiative transfer – methods: numerical – stars: emission-line, Be – stars: black holes – binaries: spectroscopic

---

## 1. Introduction

Interpreting the radiation emerging from stellar or planetary atmospheres is key to understanding our Universe as a whole, where deep insight into the underlying physics of an observed object can be obtained by analysing the electromagnetic spectrum of the emitting object. Decoding the information stored within a spectrum can be considered as a three-step process. Firstly, the emitting gas needs to be modelled numerically, which generally involves the solution of the full (radiation)-hydrodynamics equations with appropriate initial and boundary conditions, and including chemical kinetics. Secondly, the emergent spectrum needs to be calculated by solving the equation of radiative transfer for many frequencies and directions to obtain the emergent flux. Finally, the numerically

calculated (synthetic) spectrum needs to be compared with the observed one, yielding an estimate of the underlying physical state of the gas.

This general procedure, however, is computationally very challenging. The solution of the full radiation-hydrodynamics equations, for instance, constitutes already a 7-dimensional problem (three spatial dimensions, one time dimension, and for the radiative transfer one frequency/wavelength dimension if non-LTE effects are excluded and two angular dimensions). Moreover, the coupling of radiation and the state of the gas in full NLTE (non local-thermal-equilibrium) complicates the situation even further, requiring sophisticated iteration techniques via the so-called accelerated  $\Lambda$ -iteration. Thus, state-of-the-art spectral analysis tools rely on various approximations. In the OB-star regime, for instance, atmospheric modelling codes typically assume a static and spherically symmetric gas with an often prescribed parametrised velocity field (e.g. PHOENIX: Hauschildt 1992; CMFGEN: Hillier & Miller 1998, Hillier 2012; WM-BASIC: Pauldrach et al. 2001; PoWR: Hamann & Gräfener 2003, Sander et al. 2017; FASTWIND: Sundqvist & Puls 2018, Puls et al. 2020).

While these codes are very powerful in deducing the fundamental stellar parameters of OB stars (such as  $L_*$ ,  $T_{\text{eff}}$ ,  $R_*$ ,  $\dot{M}$ ), they all suffer from primarily one caveat, namely when geometrical effects induced by magnetic fields, surface and wind distortions from rotation, surrounding discs, and binarity effects play a significant role. Due to the complexity of including full NLTE calculations within multi-D geometries with supersonic velocity fields, corresponding spectral synthesis codes are only gradually developed (e.g. HDUST: Carciofi & Bjorkman 2006; PHOENIX/3D: Hauschildt & Baron 2006; WIND3D: Lobel & Blomme 2008; MAGRITTE: De Ceuster et al. 2020a, De Ceuster et al. 2020b; and a code developed by Hennicker et al. 2020).

On the other hand, when the atomic level populations are known (for instance obtained by such codes), the synthetic spectra can be calculated by solving the equation of radiative transfer along the direction to the observer in a cylindrical coordinate system (Lamers et al. 1987, Busche & Hillier 2005, Sundqvist et al. 2012, see also Hennicker et al. 2018), and the emergent flux spectrum is thus determined. This last step, that is the calculation of the so-called ‘formal integral’ is the topic of this paper. At first, we review the basic formalism for single objects and then extend this method to a detailed radiative transfer solution framework for binary systems accounting for rays propagating through the atmospheres of both objects. Finally, we apply the newly developed code to the LB-1 system, which shows a clear anti-phase behaviour of stellar absorption lines against the line wings of a broad  $H_\alpha$  emission (Liu et al. 2019).

## 2. The formal integral

As pointed out above, we are considering only the formal integral in this paper, that is, we assume the opacities and emissivities to be known, and then aim at solving the equation of radiative transfer for many frequencies to obtain the emergent fluxes. For unresolved objects at large distances, we consider only parallel rays in the direction to the observer. For a given object described in a spherical coordinate system (the object’s system),  $\Sigma_{\text{spc}}^{(\text{obj})}$ , we define a cylindrical coordinate system  $\Sigma_{\text{cyc}}^{(\text{ray})} = (p, \zeta, \tilde{z})$  in which the equation of radiative transfer will be discretized (see also Fig. 1). For each impact parameter  $p$  and polar angle  $\zeta$ , the discretization is described through the so-called  $pz$ -geometry along the  $\tilde{z}$ -axis by calculating the intersection points of the ray with the object’s spherical grid. With the discretization in the cylindrical coordinate system thus given, all coordinates are transformed to the object’s spherical system, and the required information (i.e. opacities, emissivities, and velocity fields) are interpolated onto the ray coordinates.

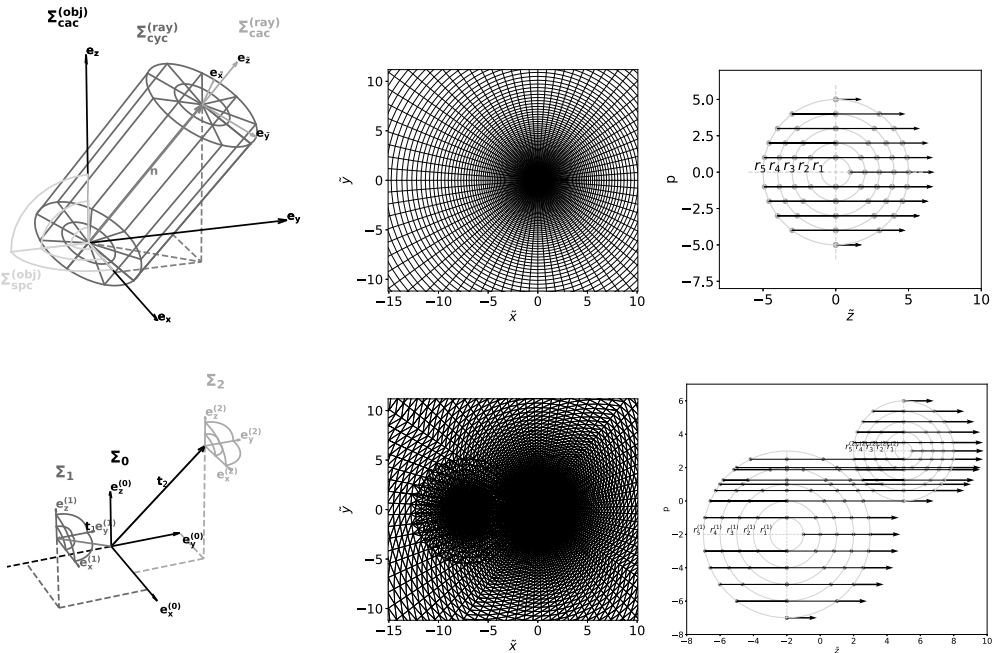


**Figure 1.** Geometry used for the formal integral. Top left panel: The object’s spherical coordinate system  $\Sigma_{\text{cyc}}^{(\text{obj})}$  (light grey) with corresponding Cartesian reference frame  $\Sigma_{\text{cac}}^{(\text{obj})}$  (black), and the ray’s cylindrical coordinate system  $\Sigma_{\text{cyc}}^{(\text{ray})}$  (dark grey) with corresponding Cartesian reference frame  $\Sigma_{\text{cac}}^{(\text{ray})}$  (grey) for an observer’s direction  $\mathbf{n} \parallel \mathbf{e}_z$ . Top middle panel: The  $p - \zeta$  (or  $\tilde{x} - \tilde{y}$ -plane) of the cylindrical coordinate system (perpendicular to the observer’s direction). Top right panel: An arbitrary  $p - \tilde{z}$ -slice, with  $\mathbf{e}_z$  pointing towards the observer. The radial grid of the spherical coordinate system is indicated by the grey circles, and the individual rays for each impact parameter  $p$  is shown by the black arrows. The radiative transfer is then performed along each ray with corresponding discretized  $\tilde{z}_k$  coordinates indicated by the grey dots. Bottom left panel: Similar to the top left panel, with two object’s coordinate systems  $\Sigma_1$  and  $\Sigma_2$  indicated by the dark grey and light grey quarter-circles, embedded within a global coordinate system  $\Sigma_0$ . The vectors  $\mathbf{t}_1$  and  $\mathbf{t}_2$  describe the origin of the local coordinate systems in the global coordinate system. Bottom middle panel: As top middle panel, however showing the triangulation of the  $\tilde{x} - \tilde{y}$ -plane for an arbitrary orbital configuration in a global cylindrical coordinate system. Bottom right panel: As top right panel, but now for the binary system with the individual  $\tilde{z}$ -rays propagating through the system of object 1 (dark grey) and object 2 (light grey). Adapted from Hennicker *et al.* (2021).

To account for non-monotonic projected velocities along the ray, we apply a grid refinement of ray coordinates if required. In the observer’s frame, the (time-independent) equation of radiative transfer is then easily solved for a given frequency, with appropriate boundary conditions for the specific intensity set here to the Planck function (or a photospheric line profile) if the ray hits the stellar core, and zero otherwise (thus neglecting the cosmic microwave background). We emphasize that Doppler shifts arising from (non-relativistic) velocity fields are automatically accounted for within the observer’s frame formulation. Thus, by solving the equation of radiative transfer for many frequencies and by integrating the emergent intensities over the projected disc at large  $\tilde{z}$ , we obtain the emergent flux profile, or accordingly the corresponding line profile.

For binary systems, we can essentially apply the very same idea as above, where now each individual object in the system is described by its own spherical coordinate system,  $\Sigma_1$  and  $\Sigma_2$ , which are embedded in a global coordinate system,  $\Sigma_0$  (see Fig. 1). For each

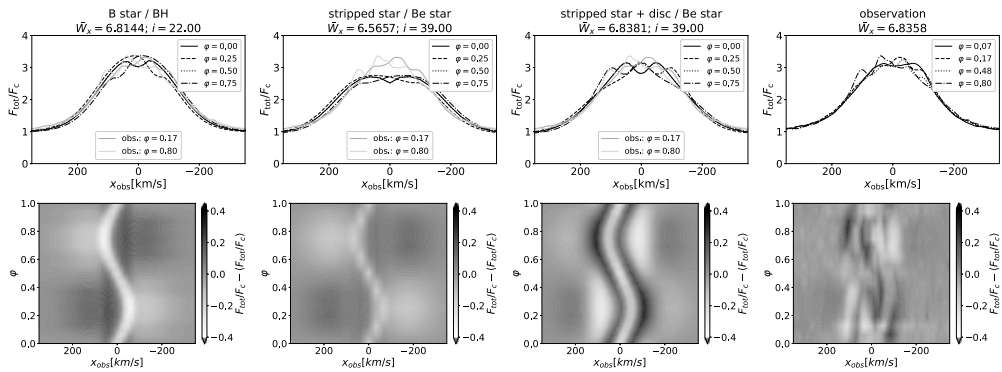


**Figure 2.**  $H_{\alpha}$  line profiles at different phases  $\varphi$  (top row) with corresponding mean-subtracted dynamical spectra (bottom row), where  $x_{\text{obs}}$  describes the frequency shift from line centre in velocity space. The first three columns to the left display the solution for three different models, (primary: B star, secondary: black hole), (primary: stripped star, secondary: Be-star), (primary: stripped star + disc, secondary: Be-star), with  $H_{\alpha}$  line profiles at two distinct phases from the actual observations indicated by the grey lines. The right column additionally displays the corresponding observed (see Shenar et al. 2020)  $H_{\alpha}$  line profiles and mean-subtracted dynamical spectrum of LB-1. All observed line profiles have been convolved with a Gaussian filter of width  $10 \text{ km s}^{-1}$  to reduce the noise. The phase-averaged equivalent width evaluated in velocity space in units of  $100 \text{ km s}^{-1}$ ,  $\bar{W}_x$ , and the inclination,  $i$ , used within the synthetic-spectra calculations are indicated at the top. Adapted from Hennicker et al. (2021).

object, we again define individual cylindrical coordinate systems which are merged in a global cylindrical system where the equation of radiative transfer will be solved. Thus, the coordinate representation of the global cylindrical system within each individual object's system can be found by simple coordinate transformations, and all required quantities are again interpolated onto each ray. The emergent fluxes are then calculated by numerically integrating the emergent specific intensities over the triangulated area of the global cylindrical coordinate system.

Since the individual coordinate systems can have completely different length-scales (which are automatically accounted for by the transformation matrices), we are able to calculate synthetic line profiles for a variety of systems, ranging from transit spectra of planetary atmospheres, to post-asymptotic giant branch binaries including circumstellar and circumbinary discs and massive-star binaries with stellar winds and disc systems.

### 3. The LB-1 system

As a first application of the developed BOSS-3D code, we consider the enigmatic binary (or multiple) system LB-1. Among other hypotheses, this system has been proposed to consist of either a B-star/black-hole (BH, Liu et al. 2019) or a stripped-star/Be-star binary (Shenar et al. 2020). From an observational point of view (see also Fig. 2), there is a clear anti-phase behaviour of the  $H_{\alpha}$  line wings against the line core. This manifests in the mean-subtracted dynamical profile, where the line wings are moving to the blue (left) side at phases  $\varphi \in [0, 0.5]$  while the line core is moving to the red (right) side.

Based on these observations, we aim at modelling the LB-1 system within BOSS-3D focussing on the two above mentioned hypotheses. To this end, we use a parametrised form of the Shakura-Sunyaev  $\alpha$ -disc model (see Shakura & Sunyaev 1973) based on Carciofi & Bjorkman (2006) for both the BH-accretion disc and the Be-decretion disc. Essentially, we assume Keplerian rotation and vertically hydrostatic equilibrium, with the temperature stratification either given from a blackbody reprocessing disc (for the Be-decretion disc) or assumed to be constant (for the BH-accretion disc). Further, we

calculate  $H_\alpha$  opacities and emissivities from Saha-Boltzmann statistics – assuming hence LTE – and use photospheric line profiles obtained from FASTWIND for all involved objects (i.e. for the B-star in the B-star/BH hypothesis, and for both the stripped star and Be-star in the other one) as an inner boundary condition of the specific intensity when the rays are crossing the stars.

For such models, we explore the disc’s parameter space by calculating a variety of dynamical  $H_\alpha$  line profiles with the BOSS-3D code. Fig. 2 shows the best-fit models. While the B-star/BH binary gives a good reproduction of the qualitative shape of  $H_\alpha$  line profiles, this model cannot reproduce the anti-phase behaviour of line wings against line core. This is somewhat obvious, since the emission part solely originates from the BH-accretion disc, thus following the BH orbit. Similarly, the stripped-star/Be-star model cannot reproduce the observed anti-phase behaviour either, since the  $H_\alpha$  emission now is following the Be-star orbit.

When introducing an (artificial) disc around the stripped star, however, both the qualitative shape of the  $H_\alpha$  line profiles as well as the dynamical spectrum is in remarkable good agreement with the observations. Though speculative, this disc might be a remnant from previous mass-transfer phases or could have been formed from re-accretion of material from the Be-star disc. We emphasize that a similar good fit can also be found when introducing a disc-disc system within the B-star/BH hypothesis as well. Thus, while we cannot rule out the one or other hypothesis, our findings still suggest that LB-1 hosts two discs.

#### 4. Summary

In this paper, we have presented a 3D radiative transfer code for binary systems (BOSS-3D), which calculates synthetic line profiles for given source and sink terms. By describing each object in the system within individual coordinate systems, BOSS-3D can handle completely different length-scales of the involved objects without loss of spatial resolution, and can be easily extended to triple or multiple systems. Moreover, by solving the radiative transfer equation in the observer’s frame, BOSS-3D can easily handle (arbitrary, but non-relativistic) supersonic velocity fields. BOSS-3D then requires the density, temperature, velocity field, opacities, and emissivities in the rest frame of each object as input, and gives the synthetic line profile(s) as output.

As a first application of BOSS-3D, we considered the LB-1 system focussing on two hypotheses (i.e. the B-star/BH and the stripped-star/Be-star hypotheses previously proposed in the literature). The observed phase-dependent  $H_\alpha$  line profiles, however, can only be reproduced when introducing a second disc in the system. Thus, our findings provide strong evidence that LB-1 contains a disc-disc system, with an additional disc either attached to the B star in the B-star/BH scenario or to the stripped star in the stripped-star/Be-star scenario.

#### References

- Busche, J. R. & Hillier, D. J. 2005, *AJ*, 129, 454  
 Carciofi, A. C. & Bjorkman, J. E. 2006, *ApJ*, 639, 1081  
 De Ceuster, F., Homan, W., Yates, J., et al. 2020, *MNRAS*, 492, 1812  
 De Ceuster, F., Bolte, J., Homan, W., et al. 2020, *MNRAS*, 499, 5194  
 Hamann, W. R. & Gräfenor, G. 2003, *A&A*, 410, 993  
 Hauschildt, P. H. 1992, *J. Quant. Spec. Radiat. Transf.*, 47, 433  
 Hauschildt, P. H. & Baron, E. 2006, *A&A*, 451, 273  
 Hennicker, L., Puls, J., Kee, N. D., & Sundqvist, J. O. 2018, *A&A*, 616, A140  
 Hennicker, L., Puls, J., Kee, N. D., & Sundqvist, J. O. 2020, *A&A*, 633, A16  
 Hennicker, L., Kee, N. D., Shenar, T., et al. 2021, *A&A*, accepted, *arXiv:2111.15345*

- Hillier, D. J. & Miller, D. L. 1998, *ApJ*, 496, 407
- Hillier, D. J. 2012, in *From Interacting Binaries to Exoplanets: Essential Modeling Tools*, ed. M. T. Richards & I. Hubeny, 282, 229–234
- Lamers, H. J. G. L. M., Cerruti-Sola, M., & Perinotto, M. 1987, *ApJ*, 314, 726
- Liu, J., Zhang, H., Howard, A. W., et al. 2019, *Nature*, 575, 618
- Lobel, A. & Blomme, R. 2008, *ApJ* 678, 408
- Pauldrach, A. W. A., Hoffmann, T. L., & Lennon, M. 2001, *A&A*, 375, 161
- Puls, J., Najarro, F., Sundqvist, J. O., & Sen, K. 2020, *A&A*, 642, A172
- Sander, A. A. C., Hamann, W. R., Todt, H., Hainich, R., & Shenar, T. 2017, *A&A*, 603, A86
- Shakura, N. I. & Sunyaev, R. A. 1973, *A&A*, 500, 33
- Shenar, T., Bodensteiner, J., Abdul-Masih, M., et al. 2020, *A&A*, 639, L6
- Sundqvist, J. O., ud-Doula, A., Owocki, S. P., et al. 2012, *MNRAS*, 423, L21
- Sundqvist, J. O. & Puls, J. 2018, *A&A*, 619, A59